Int J Clin Exp Med 2019;12(4):3340-3351
www.ijcem.com /ISSN:1940-5901/IJCEM0073876

Original Article

Pathways and protective mechanisms for cerebral ischemia-reperfusion injuries in mice

Hao Wang, Dongyuan Liu, Hongbing Zhang

Department of Neurosurgery, Beijing Luhe Hospital, Capital Medical University, Beijing, China

Received December 16, 2017; Accepted November 6, 2018; Epub April 15, 2019; Published April 30, 2019

Abstract: Ischemia-reperfusion injury (IRI) correlates with many signaling cascades. To further explore the deregulated genes and pathways involved in IRI, microarray data of GSE23163 was downloaded from Gene Expression Omnibus (GEO). Bioinformatic re-analysis was then performed. One-way analysis of variance testing was employed to obtain differentially expressed genes (DEGs) in 64 samples of the striatum and cortex from wild-type (WT) and glutathione peroxidase-1 knockout ($Gpx1^{-/-}$) mice at 0 hours (Sham control), 2 hours, 8 hours, and 24 hours postreperfusion, with *p*-value < 0.05 as the cutoff. Weighted Gene Co-expression Network Analysis (WGCNA) algorithm was employed to analyze gene co-expression modules. Functional and pathway enrichment analysis was performed for the DEGs in the most relevant modules. DEGs in the cortex and striatum of WT mice, respectively, were 3,793 and 3,963. Those for $Gpx1^{-/-}$ mice, respectively, were 4,720 and 4,719. The algorithm separately employed for the four DEG sets led to the identification of 8, 10, 12, and 7 co-expression modules, respectively. DEGs in the WT mice related to mitogen-activated protein kinase, vascular endothelial growth factor (VEGF), and toll-like receptor (TLR) signaling pathways. Those in $Gpx1^{-/-}$ mice related to lysosomes, B-cell receptor signaling pathways, VEGF, and TLR signaling pathways. In conclusion, DEGs in WT and $Gpx1^{-/-}$ mice were related to different functions and pathways. Gpx1 may play a crucial regulatory role in cerebral IRI, particularly through regulation of glutathione metabolism, phosphatidylinositol signaling system, lysosomes, and B-cell receptor signaling pathways.

Keywords: Ischemia-reperfusion injury, postreperfusion, pathway, co-expression, Gpx1

Introduction

Numerous studies have revealed that ischemia-reperfusion injuries (IRI) result in dysfunction of the brain, kidneys, liver, and so forth [1]. Of these, cerebral IRI is a common and life-threatening cerebrovascular disease with severe morbidity and mortality. Rapid reperfusion is critical in the treatment of unexpected cerebral ischemic incidents [2]. However, occurrence of postreperfusion lesions has been correlated with malignancies of brain injuries and inflammatory response [3]. A chain reaction of signaling cascades, such as inflammation, apoptosis, and necrosis, occurs after IRIs. This ultimately manifests in the loss of neuron activity and deficits of memory and motor skills [4].

A large body of mediators and pathways have been proposed to be involved in IRI, such as mitogen-activated protein kinase (MAPK) signaling pathway [2], phosphatidylinositol 3-kinase (P13K) pathway [5, 6], vascular endothelial growth factor (VEGF) signaling pathway, vascular endothelial growth factor (VEGF) signaling pathway [7, 8], and toll-like receptor (TLR) signaling pathway [9]. Arslan et al. reported that exosome treatment for C57B16/J mice with IRI increased levels of ATP, NADH, phosphorylated(p)-Akt, and p-GSK-3β, while reducing levels of p-c-Jun NH_2-terminal kinases (JNKs, one of MAPKs) and oxidative stress in IRI hearts. The infarct size in cardiovascular was reduced by 45% [5]. This protection has been associated to the activation or phosphorylation of MAPKs, such as extracellular signal-regulated kinases (ERKs) and p38 MAPK that are related to pro-inflammatory cytokines, including interleukin 1β (IL-1β) and tumor necrosis factor α (TNF-α) [2]. Inhibition of these factors and pathways has been proven to be protective to brain injuries. The addition of exogenous glutamine enha-

nces myocardial function after IRI [10]. Despite these advances in the understanding of IRI, the pathogenesis of IRI remains unclear.

Chen et al. performed a microarray analysis on the infarct cortex of wild type (WT) mice and glutathione peroxidase-1 knockout ($GPX1^{-/-}$) mice at 8 hours and 24 hours postreperfusion [11]. They found that 70% of the differentially expressed genes (DEGs) in WT mice cortexes were overlapped with that of $Gpx1^{-/-}$ mouse cortexes. They also demonstrated the crucial protective roles of GPX1 during IRI, particularly through the downplay of Nrf2-mediated cytoprotective pathways and ubiquitin-proteasome system dysfunction (UPS) function. Weighted Gene Co-expression Network Analysis (WGCNA) can effectively integrate gene expression and trait data (time and drug doses) to identify significantly related pathways and candidate biomarkers [12]. Secondary analysis of existing data is a cost-efficient way to enhance the overall efficiency of data, providing a more nuanced assessment of the primary results from the original study using different analysis methods [13]. To identify more genes that are significantly dysregulated post-reperfusion and explore the associated pathways, the present study reanalyzed the microarray data of GSE23163 deposited in the Gene Expression Omnibus (GEO) by Chen et al. [11]. DEGs were first identified in the cortex and striatum of WT and $Gpx1^{-/-}$ mice. After WGCNA algorithm analysis, functional and pathway enrichment analysis was conducted for the DEGs of WT mice and $Gpx1^{-/-}$ mice. Functions and pathways associated with the DEGs of both mice or exclusive to $Gpx1^{-/-}$ mice were examined, aiming to provide new insight into the mechanisms and processes of cerebral IRI.

Materials and methods

Microarray data and data processing

Gene expression microarray data of GSE23163, deposited in the National Center of Biotechnology Information (NCBI) GEO (http://www.ncbi.nlm.nih.gov/geo/), based on the platform of GPL6885 Illumina MouseRef-8 v2.0 expression BeadChip, were downloaded. The data consisted of 64 samples obtained from both the striatum and cortex of 4 WT and 4 $Gpx1^{-/-}$ mice at 0 hours (Sham control), 2 hours, 8 hours, and 24 hours postreperfusion, respectively. Four biological replicates were obtained for each time point.

The robust multiarray average (RMA) algorithm in Affy package of R was used for microarray data preprocessing [14], including background correction, quantile normalization, and probe summarization. If there were multiple probe sets that corresponded to the same gene, the average value of probes was calculated as the expression value of this gene. The probe was filtered if it corresponded to more than one gene.

Identification of DEGs

Detection of gene expression pattern changes in different tissues (including the striatum and cortex) of WT and $Gpx1^{-/-}$ mice within 24 hours after cerebral IRI was performed, respectively, using one-way analysis of variance (ANOVA) testing [15]. The significant cut-off criterion for differentially expressed genes (DEGs) was set at p-value < 0.05.

Gene co-expression networks analysis

WGCNA algorithm [16] is a systems biology analysis method used to construct gene sets or modules from observed gene expression data. Based on the topological overlap dissimilarity measure, WGCNA clusters the genes into modules using the network distance coupled with hierarchical clustering. Modules (clusters) are denoted by colors, which are dependent upon the number of genes within the modules. A grey color denotes genes outside of the module. Module memberships (MM) represent the correlation between the expression value of a given gene and the module eigengene (ME) (the average expression value of genes within a module), quantifying how close a gene is to a given module.

In this study, WGCNA was separately employed according to mice species and positions of chips, aiming to analyze gene co-expression networks of the DEGs obtained by ANOVA testing, with a significant mean detection level of $P < 0.05$. Gene modules related to the time series were obtained.

Functional and pathway enrichment analysis

Gene Ontology (GO) analysis is frequently used to for gene annotation of large-scale genomic

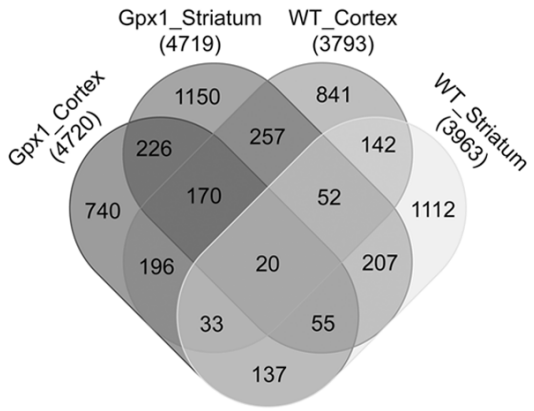

Figure 1. Differentially expressed genes (DEGs) in mice. The number in overlap square represents gene was significantly altered in samples overlapped there. WT, wild type mouse.

or transcriptomic data [17], while Kyoto Encyclopedia of Genes and Genomes (KEGG) pathway database informs people of how molecules or genes work [18]. In this study, the Database for Annotation, Visualization, and Integrated Discovery (DAVID) [19] was employed to perform GO functional and KEGG pathway enrichment analysis for time series genes obtained by the WGCNA algorithm. Remarkable GO category and KEGG pathway items were examined.

Results

Identification of DEGs

A total of 25,697 probes were included in the original microarray data of GSE23163 deposited in the NCBI database. After data preprocessing, 18,109 genes were identified. Through one-way ANOVA testing, the number of DEGs identified in WT mice, respectively, was 3,793 and 3,963. There were 247 DEGs shared by the two tissues. On the other hand, for $Gpx1^{-/-}$ mice, 4,719 DEGs were found in the striatum and 4,720 were identified in the cortex. The amount of co-expressed DEGs between the striatum and cortex for $Gpx1^{-/-}$ mice was 471. As shown in **Figure 1**, it was found that there were 334 DEGs shared by the striatum of the WT and $Gpx1^{-/-}$ mice, with 419 common DEGs in the cerebral cortex of the WT and $Gpx1^{-/-}$ mice, respectively. Expression of only 20 DEGs was significantly altered in the WT and $Gpx1^{-/-}$ mice, including mitogen-activated protein kinase (MAPK) family members MAPK 4 and MAPK6 (data not shown). Results indicated specificity of gene expression in different tissues and different mice after cerebral IRI.

Gene co-expression networks

WGCNA was applied separately to the above DEGs of WT mice and $Gpx1^{-/-}$ mice. Hierarchical clustering was separately employed to DEGs sets for the WT mice cortex, WT mice striatum, $Gpx1^{-/-}$ mice cortex, and $Gpx1^{-/-}$ mice striatum, leading to the identification of 8, 10, 12 (including the grey module), and 7 co-expression modules (**Figure 2**), respectively. The most relevant modules to the four gene sets at 0 hours, 2 hours, 8 hours, and 24 hours postreperfusion were different. According to analysis, it was found that expression of 1,711, 1,758, 1,577, and 2,137 genes were significantly altered in the WT mice cortex, WT mice striatum, $Gpx1^{-/-}$ mice cortex, and $Gpx1^{-/-}$ mice striatum at 2-24 hours postreperfusion, respectively. Most of those DEGs were upregulated or downregulated at 24 hours post-reperfusion (**Table 1**).

Function and pathway enrichment analysis for DEGs in most relevant modules

Results of GO analysis for the 1,711 DEGs in WT mice cortexes within 24 hours postreperfusion indicated that they were mainly associated with intracellular signaling cascades, lymphocyte activation during immune response, leukocyte activation during immune response, regulation of cell proliferation, and response to wounding (**Figure 3**). These DEGs were significantly involved in 9 pathways, with $P < 0.05$, including MAPK signaling pathways (TGFBR2, FGFR2, FGF2, FGF5, and MAP3K4), ribosome (RPL18 and RPL17), glutathione metabolism (GPX1 and GPX7), phosphatidylinositol signaling system (DGKB and INPPL1), and vascular endothelial growth factor (VEGF) signaling pathways (MAPK11, BAD, and RAC) (**Table 2**).

The 1,758 DEGs in WT mice striatum were correlated with the GO categories of phosphate metabolic process, phosphorylation, generation of precursor metabolites and energy, intracellular signaling cascades, protein catabolic process, and regulation of cell death (**Figure 4**). Moreover, these genes were significantly involved in 9 pathways, with $P < 0.05$, including MAPK signaling pathways (TGFBR1, MAP3K4, MAPK3, and MAPK14), ubiquitin mediated proteolysis (UBE3B and UBE2F), and toll-like rece-

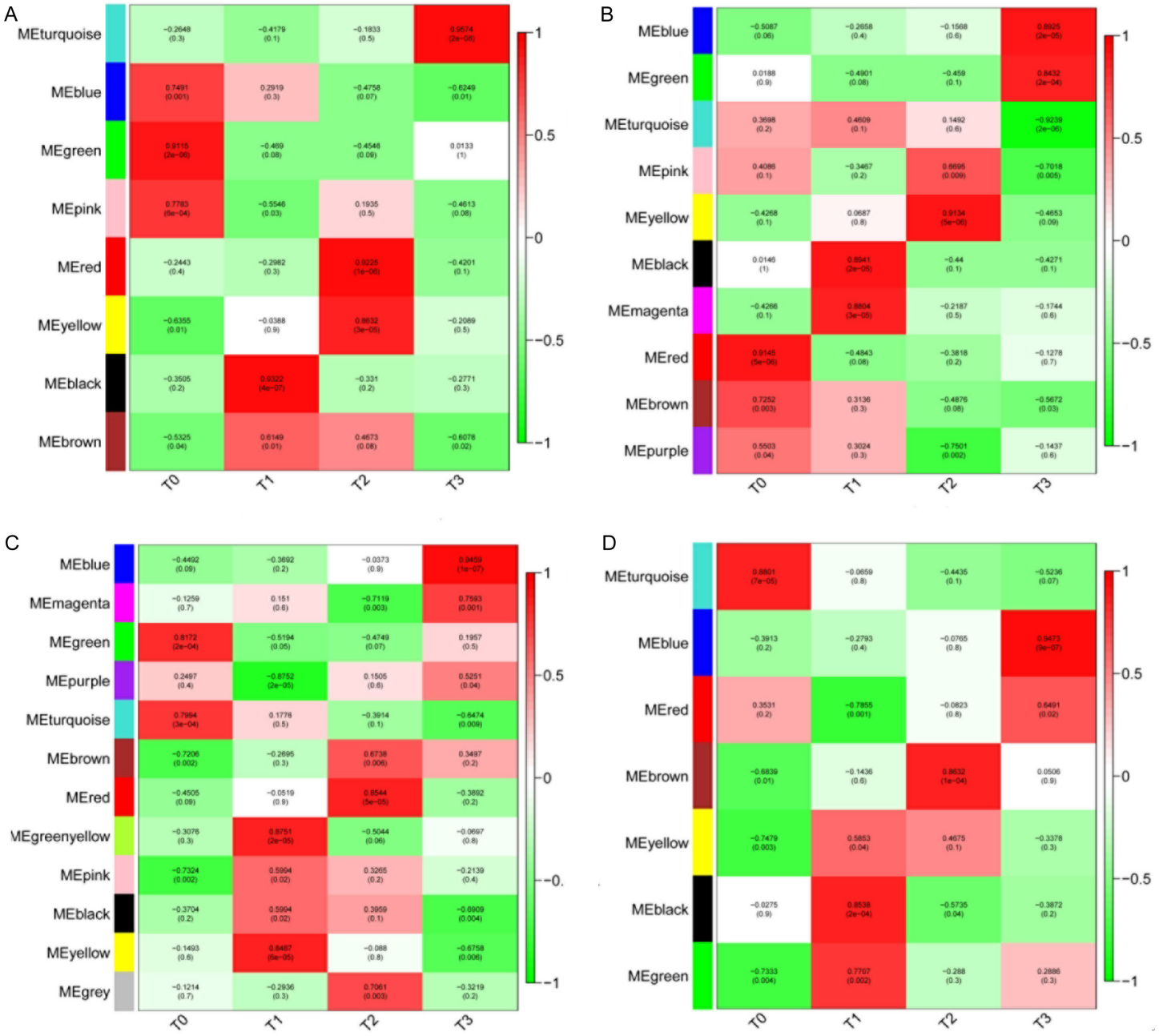
A
MEturquoise
MEblue
MEgreen
MEpink
MEred
MEyellow
MEblack
MEbrown
T0
T1
T2
T3
1
0.5
0
−0.5
−1
B
MEblue
MEgreen
MEturquoise
MEpink
MEyellow
MEblack
MEmagenta
MEred
MEbrown
MEpurple
C
MEblue
MEmagenta
MEgreen
MEpurple
MEturquoise
MEbrown
MEred
MEgreenyellow
MEpink
MEblack
MEyellow
MEgrey
D
MEturquoise
MEblue
MEred
MEbrown
MEyellow
MEblack
MEgreen

Figure 2. Co-expression modules for differentially expressed genes (DEGs) sets classified by WGCNA. A-D: Co-expression modules for DEGs sets for wild type mice right striatum, wild type mice cortex, Gpx1$^{-/-}$ mice right striatum, and Gpx1$^{-/-}$ mice cortex, respectively. Each row represents a module (labeled by color) and each column represents a trait and the time point. The value at the top of each square represents the correlation coefficient between the module eigengene and the time trait and this in parenthesis was Pearson's correlation value. The red color in the square represents positive correlation between the module eigengene and time trait and green color represents negative correlation between them. ME, module membership.

Table 1. The most relevant modules and number of genes in the striatum and cerebral cortex of wild-type mice and Gpx1$^{-/-}$ mice at different periods postreperfusion

Time postreperfusion	WT Cortex (1711)[a]		WT Striatum (1758)		Gpx1$^{-/-}$ Cortex (1577)		Gpx1$^{-/-}$ Striatum (2137)	
	Module[b]	Count[c]	Module	Count	Module	Count	Module	Count
T1 (2 h)	Black[d] (0.93; 4.22E-07)[e]	154	Black (0.89; 1.61E-05)	156	Purple (-0.87; 1.93E-05)	45	Black (0.85; 2.04E-04)	107
T2 (8 h)	Red (0.92; 9.78E-07)	187	Yellow (0.91; 5.04E-06)	446	Red (0.85; 5.00E-05)	203	Brown (0.86; 1.44E-04)	789
T3 (24 h)	Turquoise (0.96; 2.19E-08)	1370	Turquoise (-0.92; 2.38E-06)	1156	Blue (0.95; 1.00E-07)	1329	Blue (0.94; 8.98E-07)	1241

CC, correlation coefficients between the module eigengenes and the traits; *P*-value, Pearson's correlation values; WT, wild type mouse; T0-3, time at 0 h, 2 h, 8 h, and 24 h postreperfusion, respectively. a: numbers in parentheses indicate the most relevant genes in three different periods; b: indicates the most relevant module in this period; c: indicates the number of genes contained in the module most relevant in this period; d: different modules randomly defined with different colors. e: the value in parentheses indicates the correlation coefficient between the module and the period.

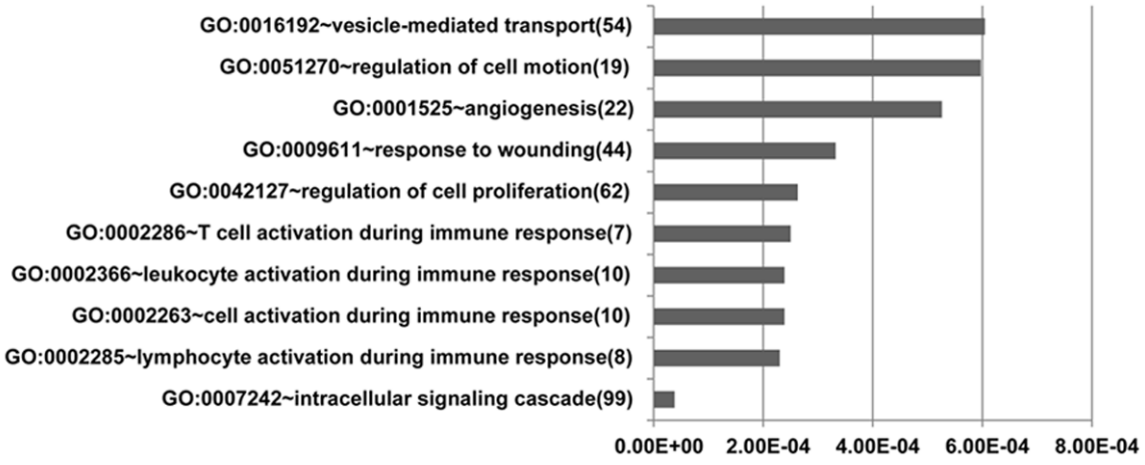

Figure 3. Top 10 of Gene Ontology (GO) categories for differentially expressed genes in wild type mice cortexes within 24 hours postreperfusion. The capital "GO" and the figure after the colon represent the GO term number. The number in the parenthesis after the GO term name was the gene count enriched in this term.

Table 2. Results of KEGG pathway analysis for differentially expressed genes in wild type mice cortex within 24 hours postreperfusion

Terms	Count	*P* Value	Gene symbols
Mmu04010: MAPK signaling pathway	37	0.001486	*FGFR2, FGF5, MKNK2, CACNB3, PPM1B, CACNB4, FGF12, ATF2, ACVR1C, TNFRSF1A, BDNF, MAP3K4, RAC2, RASGRP3, DUSP14, MAPT, PPP3CB, MOS, RRAS, NFATC4, PPP3CA, TRP53, NF1, TGFBR2, MAPK11, FGF22, CACNA2D3, FLNA, NRAS, CRKL, RPS6KA1, RPS6KA2, RAP1B, MAPK8IP1, PLA2G4B, DUSP8, DUSP6*
Mmu03010: Ribosome	17	0.002015	*RPL18, RPL17, RPL27A, RPL27, RPS27L, RPS2, RPS6, RPS5, RPL28, RPS7, RPS26, RPL21, RPL10, FAU, RPS13, RPS11, RPS27A*
Mmu04510: Focal adhesion	26	0.018292	*CAV2, CAV1, TLN1, MYL2, TLN2, SRC, VCL, RAC2, BCL2, PAK4, COL6A2, SHC3, PIK3R1, COL4A4, COL4A2, BAD, VAV1, COL4A6, FLNA, LAMA2, VEGFC, CCND1, CRKL, RAP1B, RELN, ITGA2B*
Mmu00480: Glutathione metabolism	10	0.023428	*GSTM2, GPX1, OPLAH, SRM, PGD, IDH2, ANPEP, GPX7, GSTP2, MGST1*
Mmu04666: Fc gamma R-mediated phagocytosis	15	0.027243	*DNM1L, PIP5K1B, ARPC4, VAV1, WAS, FCGR1, AMPH, ARPC1A, ARPC1B, CRKL, FCGR2B, RAC2, PLCG2, PPAP2A, PIK3R1*
Mmu04070: Phosphatidylinositol signaling system	12	0.039927	*CDS2, DGKB, INPPL1, PLCG2, PLCD3, PIP5K1B, DGKZ, SYNJ2, CDS1, ITPKA, PIK3R1, ITPR1*
Mmu05014: Amyotrophic lateral sclerosis (ALS)	10	0.039989	*TRP53, TNFRSF1A, GPX1, GRIN2B, BCL2, PPP3CB, MAPK11, PPP3CA, BAD, CASP1*
Mmu04370: VEGF signaling pathway	12	0.043403	*NRAS, RAC2, PLCG2, PPP3CB, NFATC4, NOS3, MAPK11, PPP3CA, BAD, PLA2G4B, PIK3R1, SRC*
Mmu04810: Regulation of actin cytoskeleton	26	0.048774	*FGFR2, FGF5, MYL2, PIP5K1B, ARPC4, FGF12, ITGAM, IQGAP1, VCL, PFN1, RAC2, PAK4, MOS, RRAS, MSN, PIK3R1, GIT1, FGF22, VAV1, WAS, ARPC1A, NRAS, ARPC1B, CRKL, ARAF, ITGA2B*

KEGG, Kyoto Encyclopedia of Genes and Genomes.

ptor (TLR) signaling pathways (MAPK3, MAPK-14, TLR3, and RAC1) (**Table 3**).

After analysis using DAVID, the 1,577 DEGs in Gpx1$^{-/-}$ mice cortexes were identified to be significantly related to GO categories of response to wounding, positive regulation of immune response, and positive regulation of response to stimulus (**Figure 5**). Additionally, these DEGs were connected to significantly enriched pathways, such as lysosomes (LAMP2 and CD68), TLR signaling pathways (CD14, TLR1, and CASP8), ribosome (RPL18 and RPL35A), p53 signaling pathways (CCND1, CASP9, BAX, and CASP8), and phosphatidylinositol signaling systems (PIK3CG and INPPL1) (**Table 4**).

GO analysis for DEGs in the Gpx1$^{-/-}$ mice striatum within 24 hours postreperfusion showed that 2,137 DEGs were mainly associated with

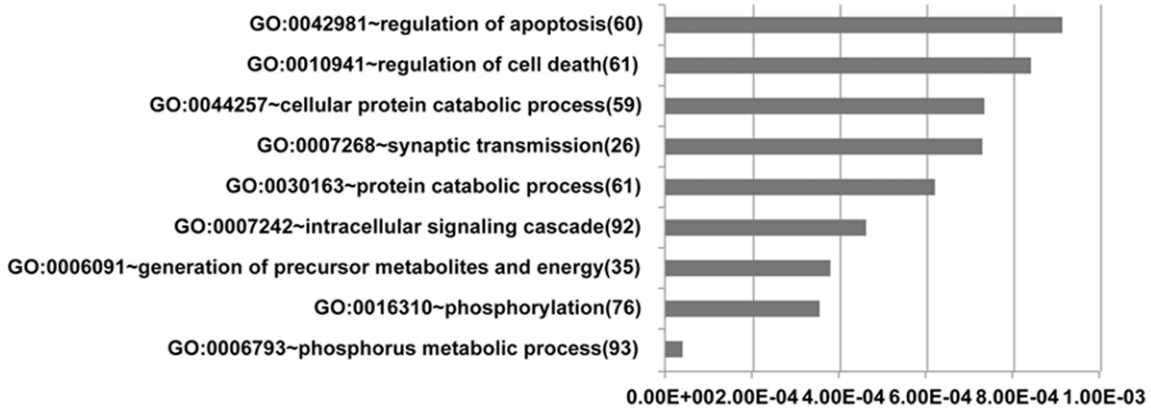

Figure 4. Top 10 of Gene Ontology (GO) categories for differentially expressed genes in wild type mice striatum within 24 hours postreperfusion. The capital "GO" and the figure after the colon represent the GO term number. The number in the parenthesis after the GO term name was the gene count enriched in this term.

Table 3. KEGG pathway analysis for differentially expressed genes in wild type mice striatum within 24 hours postreperfusion

Terms	Count	*P* Value	Gene symbols
Mmu04010: MAPK signaling pathway	33	0.00381	*PDGFB, MKNK2, MAP3K6, MAX, MAP3K4, RASGRP3, MAPT, RAC1, PRKACA, NFATC4, TRAF6, MAP2K7, RASA1, MAP2K1, TGFBR1, RELB, NF1, PTPRR, STK4, HRAS1, DUSP3, DUSP2, ARRB2, MAPK14, MAPK3, NTRK2, PDGFRA, MAPK8IP1, CACNA1C, IKBKB, CD14, MAP3K12, PPP5C*
Mmu04120: Ubiquitin mediated proteolysis	20	0.005225	*SYVN1, UBE3B, BTRC, CDC23, UBE2F, ANAPC10, CDC34, PARK2, UBE2J2, HERC2, UBE2R2, TRIM37, FANCL, CUL2, CUL5, PIAS3, WWP2, UBE2M, DDB2, TRAF6*
Mmu00450: Selenoamino acid metabolism	7	0.005498	*SEPHS2, SCLY, WBSCR22, PAPSS1, CBS, MARS, HEMK1*
Mmu00750: Vitamin B6 metabolism	4	0.006859	*PDXK, PDXP, PNPO, PSAT1*
Mmu04540: Gap junction	13	0.024086	*ADCY2, PDGFB, MAP2K1, GNA11, GRM1, HRAS1, PLCB4, MAPK3, PDGFRA, PRKACA, HTR2C, TUBB3, TUBB4*
Mmu05210: Colorectal cancer	13	0.024086	*DVL3, MSH6, MAP2K1, PIK3CB, TGFBR1, CYCS, FZD2, DVL1, CASP9, MAPK3, RAC1, PDGFRA, PIK3R1*
Mmu04620: Toll-like receptor signaling pathway	14	0.030401	*CCL3, MAP2K1, PIK3CB, TLR3, CCL4, CD86, MAPK14, RAC1, MAPK3, IKBKB, TRAF6, MAP2K7, PIK3R1, CD14*
Mmu05211: Renal cell carcinoma	11	0.032619	*CUL2, HIF1A, PDGFB, MAP2K1, PIK3CB, PAK4, RAC1, GAB1, MAPK3, PIK3R1, HRAS1*
Mmu00534: Heparan sulfate biosynthesis	6	0.04569	*B3GAT3, B3GALT6, XYLT2, HS6ST1, EXT2, HS2ST1*

KEGG, Kyoto Encyclopedia of Genes and Genomes.

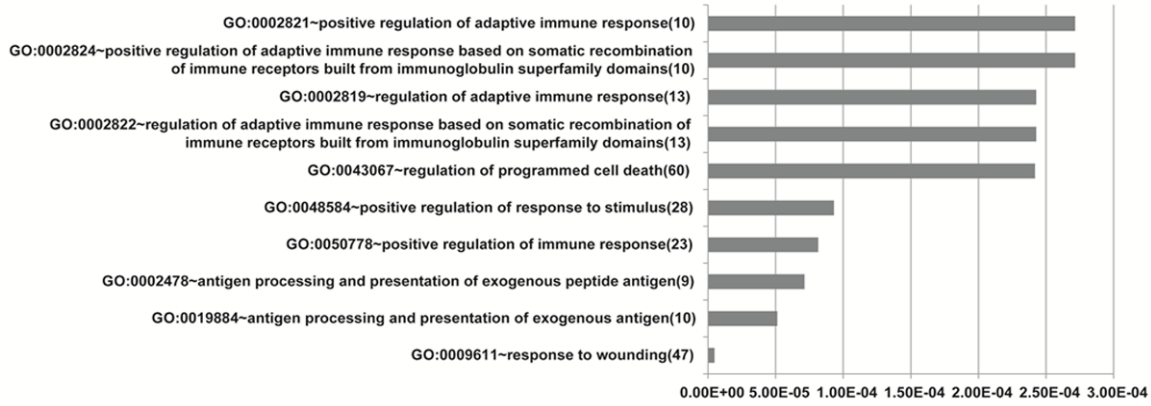

Figure 5. Top 10 of Gene Ontology (GO) categories for differentially expressed genes in Gpx1$^{-/-}$ mice cortexes within 24 hours postreperfusion. The capital "GO" and the figure after the colon represent the GO term number. The number in the parenthesis after the GO term name was the gene count enriched in this term.

Table 4. KEGG pathway analysis for differentially expressed genes in Gpx1$^{-/-}$ mice cortexes within 24 hours postreperfusion

Terms	Count	*P* Value	Gene symbols
Mmu04142: Lysosome	25	5.92E-04	*HEXA, LGMN, ACP5, PPT2, ASAH1, GLB1, SLC11A1, CD68, LAPTM5, GBA, TCIRG1, CTSZ, GUSB, NAPSA, CD164, CD63, MANBA, LAMP1, LAMP2, SMPD1, NEU1, CTSB, GGA1, CTSH, GGA3*
Mmu04620: Toll-like receptor signaling pathway	22	6.43E-04	*PIK3CG, IRAK1, IL6, PIK3CB, LY96, RELA, TLR1, TLR2, FADD, TLR6, TLR7, CXCL10, CD86, MYD88, IRF5, JUN, RIPK1, CASP8, IRF3, LBP, CD14, SPP1*
Mmu04512: ECM-receptor interaction	19	0.001174	*COL4A2, COL4A1, TNC, NPNT, COL3A1, COL2A1, SDC4, SDC2, SDC3, ITGA9, GP5, CD44, ITGB8, ITGA5, ITGA7, COL6A2, COL6A1, COL11A1, SPP1*
Mmu05212: Pancreatic cancer	16	0.004423	*PIK3CG, E2F2, RALBP1, PIK3CB, TGFBR1, ARHGEF6, RELA, TGFBR2, STAT3, TGFB1, TGFB2, CCND1, CASP9, RAC2, RAC3, RALA*
Mmu05200: Pathways in cancer	48	0.004992	*E2F2, WNT3A, MMP9, PPARG, PML, TGFB1, TPM3, TGFB2, CCNE2, CUL2, WNT4, RAC2, CASP9, RAC3, CASP8, CSF3R, RALA, RARB, FGF1, RUNX1, CSF1R, PIK3CG, RET, COL4A2, IL6, AR, COL4A1, RALBP1, PIK3CB, FLT3, RELA, TGFBR1, TGFBR2, FADD, FZD2, CTNNA1, STAT3, CDK2, HRAS1, NRAS, CCND1, PIAS4, HDAC1, BAX, JUN, RASSF1, PLCG2, PIAS1*
Mmu03010: Ribosome	18	0.00642	*RPL18, RPL35A, RPS15A, RPS27L, RPS2, RPL39, RPS6, RPS5, RPS3, RPS26, RPL30, RPS19, RPL3L, RPL10, RPS13, RPL12, RPS27A, RPL36AL*
Mmu04662: B cell receptor signaling pathway	16	0.012004	*PIK3CG, IFITM1, PIK3CB, RELA, NFKBIB, VAV1, BTK, HRAS1, NRAS, RASGRP3, FCGR2B, RAC2, RAC3, JUN, PLCG2, BLNK*
Mmu00052: Galactose metabolism	8	0.014601	*AKR1B8, B4GALT1, GALK1, AKR1B3, HK3, HK2, GALT, GLB1*
Mmu00562: Inositol phosphate metabolism	12	0.016339	*PIK3CG, CDIPT, PLCE1, PLCB3, PIK3CB, INPPL1, PLCG2, PIP5K1B, PLCD4, INPP4B, INPP4A, IPMK*
Mmu04115: p53 signaling pathway	14	0.01795	*PMAIP1, SESN2, SESN1, CDK2, CCNE2, PPM1D, CCND1, CASP9, SIAH1B, CCND2, BAX, CASP8, APAF1, IGFBP3*
Mmu04070: Phosphatidylinositol signaling system	14	0.033842	*PIK3CG, CDIPT, INPPL1, PIK3CB, PIP5K1B, CDS1, ITPR2, PLCB3, PLCE1, DGKE, PLCG2, PLCD4, INPP4B, INPP4A*
Mmu05220: Chronic myeloid leukemia	14	0.037247	*PIK3CG, E2F2, PIK3CB, TGFBR1, RELA, TGFBR2, TGFB1, TGFB2, PTPN11, HRAS1, NRAS, CCND1, HDAC1, RUNX1*
Mmu04640: Hematopoietic cell lineage	15	0.038217	*IL6, IL1R1, CD3E, FLT3, CD24A, IL11, CD9, GP5, CD44, CD34, ITGA5, CD2, CSF3R, CD14, CSF1R*
Mmu01040: Biosynthesis of unsaturated fatty acids	7	0.047056	*PECR, ACOT7, SCD2, PTPLB, FADS1, FADS2, ELOVL6*
Mmu04210: Apoptosis	15	0.049424	*PIK3CG, IRAK1, IL1R1, PIK3CB, CSF2RB2, RELA, FADD, TNFRSF1A, MYD88, CASP9, BAX, RIPK1, PRKAR1A, CASP8, APAF1*

KEGG, Kyoto Encyclopedia of Genes and Genomes.

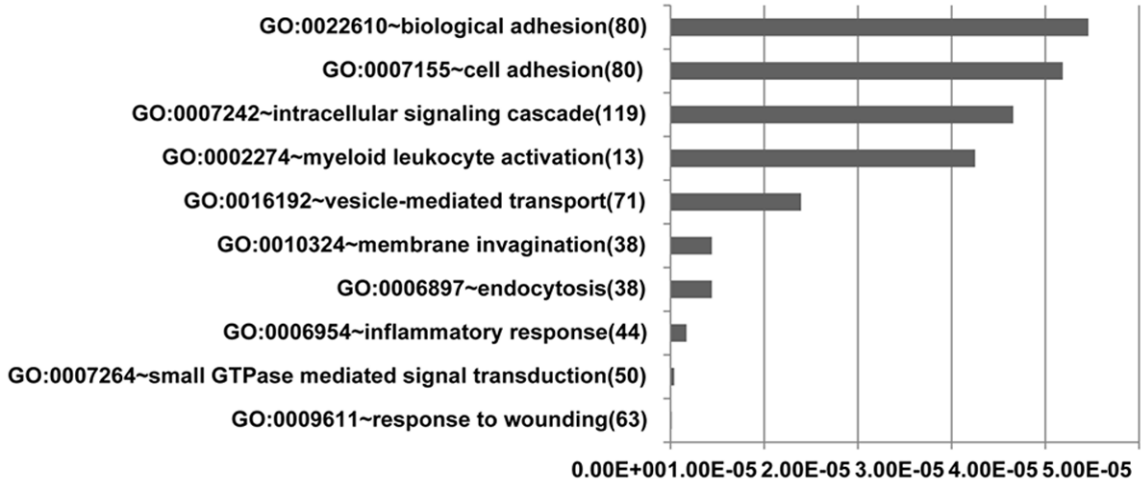

Figure 6. Top 10 of Gene Ontology (GO) categories for differentially expressed genes in Gpx1$^{-/-}$ mice striatum within 24 hours postreperfusion. The capital "GO" and the figure after the colon represent the GO term number. The number in the parenthesis after the GO term name was the gene count enriched in this term.

Table 5. KEGG pathway analysis for differentially expressed genes in Gpx1$^{-/-}$ mice striatum within 24 hours post-reperfusion

KEGG Terms	Count	*P* Value	Genes
Mmu03030: DNA replication	10	9.68E-04	*RPA1, RFC3, SSBP1, POLE3, RFC2, POLD1, LIG1, POLA2, MCM3, MCM5*
Mmu04142: Lysosome	19	0.003785	*CLN3, ABCB9, CTSZ, AP1M1, NAGLU, AP1B1, GUSB, LGMN, SLC11A1, LAMP2, CD68, GNPTAB, CTSC, CTSB, CTSH, CLN5, ATP6V0A2, GBA, CTSF*
Mmu04360: Axon guidance	20	0.004777	*NGEF, LIMK1, EFNA3, DPYSL5, DPYSL2, FES, CDK5, SLIT2, SEMA5B, NRAS, RAC2, RAC3, UNC5A, CFL1, PPP3CB, SEMA4B, UNC5D, RHOD, SEMA3A, NFATC2*
Mmu03430: Mismatch repair	7	0.005025	*RPA1, RFC3, SSBP1, RFC2, POLD1, LIG1, PMS2*
Mmu04662: B cell receptor signaling pathway	14	0.007137	*CR2, IFITM1, VAV1, BTK, NRAS, FCGR2B, RAC2, RAC3, PLCG2, PPP3CB, PIK3AP1, CD79A, PIK3R3, NFATC2*
Mmu05212: Pancreatic cancer	13	0.007819	*RALBP1, TGFBR1, TGFBR2, SMAD4, SMAD2, STAT1, STAT3, TGFB2, CCND1, CASP9, RAC2, RAC3, PIK3R3*
Mmu04650: Natural killer cell mediated cytotoxicity	18	0.010967	*PRF1, ICAM2, ITGB2, VAV1, FCGR3, HCST, NRAS, IFNA1, RAC2, RAC3, PLCG2, PPP3CB, FCER1G, SHC1, PIK3R3, NFATC2, IFNGR1, TYROBP*
Mmu04620: VEGF signaling pathway	12	0.028657	*NRAS, MAPK12, RAC2, CASP9, RAC3, PLA2G12A, PLCG2, PPP3CB, NOS3, NFATC2, PIK3R3, KDR*
Mmu00100: Steroid biosynthesis	5	0.036166	*EBP, SC5D, LSS, SC4MOL, DHCR24*
Mmu04620: Toll-like receptor signaling pathway	14	0.037521	*IL6, TOLLIP, TLR1, FADD, TLR6, STAT1, CXCL10, IFNA1, MYD88, MAPK12, IRF3, LBP, PIK3R3, SPP1*
Mmu03420: Nucleotide excision repair	8	0.042676	*RPA1, XPA, RFC3, POLE3, RFC2, POLD1, LIG1, RBX1*

KEGG, Kyoto Encyclopedia of Genes and Genomes.

response to wounding, small GTPase mediated signal transduction, inflammatory response, and intracellular signaling cascade (**Figure 6**). These DEGs were significantly involved in lysosomes (LAMP2 and CD68), B-cell receptor signaling pathways (RAC2, RAC3, and CD79A), VEGF signaling pathways (MAPK12, RAC2, and CASP9), and TLR signaling pathways (TLR1, TLR6, and MAPK12) (**Table 5**).

Discussion

An investigation by Chen et al. reported that neuronal injuries after transient cerebral ischemia, in the presence or absence of Gpx1, present different deregulated signaling mechanisms. Gpx1$^{-/-}$ mice revealed regulation of additional novel pathways, particularly the downplay of Nrf2-mediated cytoprotective pathways, p53-mediated proapoptotic pathways, and UPS function [11]. The current study used existing data from a publicly available database deposited by Chen et al. [11], with the aim of digging its value using different analysis methods. Additionally, the present study examined signaling changes in the striatum of WT and Gpx1$^{-/-}$ mice, not only affecting signaling in the cortex. Using the threshold of p-value < 0.05 for ANOVA, this study first identified different number of DEGs in the WT mice cortex, WT mice striatum, Gpx1$^{-/-}$ mice cortex, and Gpx1$^{-/-}$ mice striatum, within 24 hours postreperfusion (0 hours, 2 hours, 8 hours, and 24 hours), respectively, indicating the specificity of gene expression in different tissues and different mice with the presence or absence of Gpx1 after cerebral IRI. Next, WGCNA analysis was used to explore the most relevant genes in the WT mice cortex, WT mice striatum, Gpx1$^{-/-}$ mice cortex, and Gpx1$^{-/-}$ mice striatum. These were then evaluated by functional enrichment analysis. Intriguingly, it was found that DEGs in the cortex and striatum of WT mice were both significantly associated with MAPK signaling pathways. However, DEGs in the tissues of Gpx1$^{-/-}$ mice were not enriched in this pathway. Ubiquitin mediated proteolysis was also enriched by the inter-time-point DEGs in the WT mice striatum after IRI. VEGF signaling pathways and TLR signaling pathways were significantly enriched by DEGs in the cortex and striatum of WT and Gpx1$^{-/-}$ mice. Moreover, DEGs in the cortex and striatum of Gpx1$^{-/-}$ mice were associated with deregulation of lysosomes and B-cell receptor signaling pathways. In accord with the study of Chen et al. [11], p53 signaling pathways were exclusive to the Gpx1$^{-/-}$ cortex.

MAPK is an integral component of cellular signaling during mitogenesis and differentiation of

mitotic cells [20]. MAPK signaling pathways, such as extracellular signal-regulated kinases (ERKs) and c-Jun NH_2-terminal kinases (JNKs), are the best known MAPKs activated after focal cerebral IRI [2]. They have positive effects on cell injuries. MAPKs function as mediators of cellular stress by activating other cytosolic proteins, transcription factors, and intracellular enzymes that are implicated in various processes, including neuronal survival or damage and inflammatory and apoptotic processes of cerebral IRI [2, 21]. Activation or phosphorylation of ERK, p38 MAPK, and JNK occurring after IRI have been related to expression of proinflammatory cytokines interleukin 1β (IL-1β) and tumor necrosis factor α (TNF-α) [2]. Additionally, inhibition of MAPKs, such as p38 MAPK [22] and JNK [23, 24], has been proven to be protective in a variety models of brain injury by reducing expression of inflammatory cytokines. DEGs in the WT mice mainly enriched into MAPK signaling pathways, including MAPK members MAPK3, MAPK11, and MAPK8IP1. Thus, it is highly likely that inhibition of these genes can provide benefits to IRI treatment. They may be therapeutic targets for IRI.

The present study found that DEGs in WT and $Gpx1^{-/-}$ mice, such MAPKs (MAPK4 and MAPK-11) and RACs (RAC1 and RAC2), were associated with VEGF and TLR signaling pathways. Moreover, DEGs in $Gpx1^{-/-}$ mice, such as MAPK-12 and RAC2, were also involved in these two pathways. TLR signaling pathways play an essential role in induction of inflammatory and immune response and tissue repair [25-28]. Inhibition of TLRs, such TLR4, attenuates myocardial IRI resulting in the reduction in p-JNK and NF-κB translocation [29, 30]. VEGF production following acute IRI and mesenchymal stem cell-associated myocardial recovery may be mediated by TLR2 [9]. Angiogenic factors VEGFs and its receptors VEGFRs are the most important angiogenesis regulators [8]. VEGF has been reported to stimulate apoptosis, as well as ERK1/2 signaling pathways and MAPKs in cerebral endothelial cells after ischemic injury [7]. It has been verified that VEGF and its receptor VEGR2 are upregulated in renal IRI [1]. Protective effects of VEGFs might be associated with MAPKs, the MAPK/PI3K-Akt/VEGF signaling pathways. Activation of VEGF could activate PI3K/Akt and ERK1/2 pathw ays and inhibition of PI3K/Akt and ERK1/2 may lead to a significant decrease of VEGF activation [31]. In the present study, cerebral ischemia in the cortex or striatum of WT and $Gpx1^{-/-}$ mice induced changes of gene expression in VEGF and TLR signaling pathways at 2-24 hours postreperfusion. These list of genes may contribute to IRI, providing new insight into the mechanisms and process of cerebral IRI.

The GPX1 gene knocked out in $Gpx1^{-/-}$ mice was significantly altered in WT mice cortexes and was associated with glutathione metabolism and phosphatidylinositol signaling system. Indeed, overexpression of Gpx1 demonstrated a greater compensatory response to cerebral IRI [32]. DEGs in WT mice were less than that in $Gpx1^{-/-}$ mice, as well as those at 2-24 hours postreperfusion. These results may be due to the protective trait of GPX1 against IRI occurring via preservation of tissue metabolism, such as glutathione metabolism and phosphatidylinositol signaling system. The preservation of glutathione is dose dependent. The addition of glutamine on rats, 18 hours before a heart excision, perfusion, exposure to global ischemia, and reperfusion, could enhance myocardial tissue metabolism and glutathione content, thus improving myocardial function after IRI [10]. Results demonstrated that GPX1, as well as glutathione metabolism, contribute greatly to the inhibition of IRI progression. On the other hand, present results showed that deregulation of lysosomes and B-cell receptor signaling pathways was exclusive to the cortex and striatum of $Gpx1^{-/-}$ mice. Evidence has shown that priming of the autophagy-lysosome machinery mediates the beneficial effects of intermittent fasting preconditions to IRI [33]. Therefore, B-cell deficiency has been shown to confer protection from renal IRI [34]. However, there has been relatively little work describing the roles of B-cells in cerebral IRI. In this study, deletion of Gpx1 led to the dysregulation of lysosomes and B-cell receptor signaling pathways, indicating that these pathways were evoked by the lack of functional Gpx1. Together, these results clearly provide data in defining the crucial regulatory roles of Gpx1 in cerebral IRI, particularly through regulation of glutathione metabolism, phosphatidylinositol signaling system, lysosomes, and B-cell receptor signaling pathways.

In conclusion, genes significantly dysregulated in WT mice and $Gpx1^{-/-}$ mice were partially iden-

tical. They were involved in different signaling pathways and functions. DEGs in WT mice mainly related to MAPK signaling pathways, VEGF signaling pathways, and TLR signaling pathways. DEGs in $Gpx1^{-/-}$ mice related to lysosomes, B-cell receptor signaling pathways, VEGF signaling pathways, and TLR signaling pathways. In addition, the present study suggests the potentially crucial regulatory roles of Gpx1 in cerebral IRI, particularly through regulation of glutathione metabolism, phosphatidylinositol signaling system, lysosomes, and B-cell receptor signaling pathways. The present may provide new insight into mechanisms and process of cerebral IRI.

Disclosure of conflict of interest

None.

Address correspondence to: Hongbing Zhang, Department of Neurosurgery, Beijing Luhe Hospital, Capital Medical University, No. 82 Xinhua South Road, Tongzhou District, Beijing 101149, China. Tel: +86-10-69543901; Fax: +86-10-69531069; E-mail: hongbingzh2016@hotmail.com

References

[1] Liu F, Lou YL, Wu J, Ruan QF, Xie A, Guo F, Cui SP, Deng ZF and Wang Y. Upregulation of microRNA-210 regulates renal angiogenesis mediated by activation of VEGF signaling pathway under ischemia/perfusion injury in vivo and in vitro. Kidney Blood Press Res 2012; 35: 182-191.

[2] Jiang M, Li J, Peng Q, Liu Y, Liu W, Luo C, Peng J, Li J, Yung KKL and Mo Z. Neuroprotective effects of bilobalide on cerebral ischemia and reperfusion injury are associated with inhibition of pro-inflammatory mediator production and down-regulation of JNK1/2 and p38 MAPK activation. J Neuroinflammation 2014; 11: 1-17.

[3] Eltzschig HK and Eckle T. Ischemia and reperfusion-from mechanism to translation. Nat Med 2011; 17: 1391-1401.

[4] De Haan JB, Bladier C, Griffiths P, Kelner M, O'Shea RD, Cheung NS, Bronson RT, Silvestro MJ, Wild S and Zheng SS. Mice with a homozygous null mutation for the most abundant glutathione peroxidase, Gpx1, show increased susceptibility to the oxidative stress-inducing agents paraquat and hydrogen peroxide. J Biol Chem 1998; 273: 22528-22536.

[5] Arslan F, Lai RC, Smeets MB, Akeroyd L, Choo A, Aguor EN, Timmers L, van Rijen HV, Doevendans PA, Pasterkamp G, Lim SK, de Kleijn DP. Mesenchymal stem cell-derived exosomes increase ATP levels, decrease oxidative stress and activate PI3K/Akt pathway to enhance myocardial viability and prevent adverse remodeling after myocardial ischemia/reperfusion injury. Stem Cell Res 2013; 10: 301-312.

[6] Ha T, Hua F, Liu X, Ma J, Mcmullen JR, Shioi T, Izumo S, Kelley J, Gao X and Browder W. Lipopolysaccharide-induced myocardial protection against ischaemia/reperfusion injury is mediated through a PI3K/Akt-dependent mechanism. Cardiovasc Res 2008; 78: 546-553.

[7] Narasimhan P, Liu J, Song YS, Massengale JL and Chan PH. VEGF Stimulates the ERK 1/2 signaling pathway and apoptosis in cerebral endothelial cells after ischemic conditions. Stroke 2009; 40: 1467-73.

[8] Shibuya M. Vascular endothelial growth factor receptor-1 (VEGFR-1/Flt-1): a dual regulator for angiogenesis. Angiogenesis 2006; 9: 225-230.

[9] Abarbanell AM, Wang Y, Herrmann JL, Weil BR, Poynter JA, Manukyan MC and Meldrum DR. Toll-like receptor 2 mediates mesenchymal stem cell-associated myocardial recovery and VEGF production following acute ischemia-reperfusion injury. Am J Physiol Heart Circ Physiol 2010; 298: H1529-36.

[10] Wischmeyer PE, Jayakar D, Williams U, Singleton KD, Riehm J, Bacha EA, Jeevanandam V, Christians U and Serkova N. Single dose of glutamine enhances myocardial tissue metabolism, glutathione content, and improves myocardial function after ischemia-reperfusion injury. Jpen J Parenter Enteral Nutr 2003; 27: 396-403.

[11] Chen MJ, Wong CHY, Peng ZF, Manikandan J, Melendez AJ, Tan TM, Crack PJ and Cheung NS. A global transcriptomic view of the multifaceted role of glutathione peroxidase-1 in cerebral ischemic-reperfusion injury. Free Radic Biol Med 2011; 50: 736-48.

[12] Presson AP, Sobel EM, Papp JC, Suarez CJ, Whistler T, Rajeevan MS, Vernon SD and Horvath S. Integrated weighted gene co-expression network analysis with an application to chronic fatigue syndrome. BMC Syst Biol 2008; 2: 95.

[13] Cheng HG and Phillips MR. Secondary analysis of existing data: opportunities and implementation. Shanghai Arch Psychiatry 2014; 26: 371-375.

[14] Irizarry RA, Hobbs B, Collin F, Beazer-Barclay YD, Antonellis KJ, Scherf U and Speed TP. Exploration, normalization, and summaries of high density oligonucleotide array probe level data. Biostatistics 2003; 4: 249-264.

[15] D S. Analysis of variance (ANOVA) calculator: one-way ANOVA from summary data [Software]. 2013.
[16] Langfelder P, Horvath S. WGCNA: an R package for weighted correlation network analysis. BMC Bioinformatics 2008; 9: 559.
[17] Hulsegge I, Kommadath A and Smits MA. Globaltest and GOEAST: two different approaches for gene ontology analysis. BMC proc 2009; 3 Suppl 4: S10.
[18] Kanehisa M and Goto S. KEGG: kyoto encyclopedia of genes and genomes. Nucleic Acids Res 2000; 27: 29-34.
[19] Dennis G Jr, Sherman BT, Hosack DA, Yang J, Gao W, Lane HC and Lempicki RA. DAVID: database for annotation, visualization, and integrated discovery. Genome Biol 2003; 4: P3.
[20] Atkins CM, Selcher JC, Petraitis JJ, Trzaskos JM and Sweatt JD. The MAPK cascade is required for mammalian associative learning. Nat Neurosci 1998; 1: 602-609.
[21] Kyriakis JM and Avruch J. Mammalian MAPK signal transduction pathways activated by stress and inflammation: a 10-year update. Physiol Rev 2012; 92: 689-737.
[22] Strassburger M, Braun H and Reymann KG. Anti-inflammatory treatment with the p38 mitogen-activated protein kinase inhibitor SB-239063 is neuroprotective, decreases the number of activated microglia and facilitates neurogenesis in oxygen-glucose-deprived hippocampal slice cultures. Eur J Pharmacol 2008; 592: 55-61.
[23] Gao Y, Signore AP, Yin W, Cao G, Yin XM, Sun F, Luo Y, Graham SH, Chen J. Neuroprotection against focal ischemic brain injury by inhibition of c-Jun N-terminal kinase and attenuation of the mitochondrial apoptosis-signaling pathway. J Cereb Blood Flow Metab 2005; 25: 694-712.
[24] Benakis C, Bonny C and Hirt L. JNK inhibition and inflammation after cerebral ischemia. Brain Behav Immun 2010; 24: 800-11.
[25] Li M, Carpio DF, Zheng Y, Bruzzo P, Singh V, Ouaaz F, Medzhitov RM and Beg AA. An essential role of the NF-kappa B/Toll-like receptor pathway in induction of inflammatory and tissue-repair gene expression by necrotic cells. J Immunol 2001; 166: 7128-35.
[26] Beg AA. Endogenous ligands of Toll-like receptors: implications for regulating inflammatory and immune responses. Trends Immunol 2002; 23: 509-512.
[27] Lin Q, Li M, Fang D, Fang J and Su SB. The essential roles of Toll-like receptor signaling pathways in sterile inflammatory diseases. Int Immunopharmacol 2011; 11: 1422-32.
[28] van Zoelen MA, Yang H, Florquin S, Meijers JC, Akira S, Arnold B, Nawroth PP, Bierhaus A, Tracey KJ and, van der Poll T. Role of toll-like receptors 2 and 4, and the receptor for advanced glycation end products in high-mobility group box 1-induced inflammation in vivo. Shock 2009; 31: 280-4.
[29] Shimamoto A, Chong AJ, Yada M, Shomura S, Takayama H, Fleisig AJ, Agnew ML, Hampton CR, Rothnie CL and Spring DJ. Inhibition of Toll-like receptor 4 with eritoran attenuates myocardial ischemia-reperfusion injury. Circulation 2006; 114: 270-274.
[30] Wei C. Toll-like receptor signaling: a critical modulator of cell survival and ischemic injury in the heart. Am J Physiol Heart Circ Physiol 2009; 296: H1-12.
[31] Adya R, Tan BK, Punn A, Chen J and Randeva HS. Visfatin induces human endothelial VEGF and MMP-2/9 production via MAPK and PI3K/Akt signalling pathways: novel insights into visfatin-induced angiogenesis. Cardiovasc Res 2008; 78: 356-65.
[32] Weisbrot-Lefkowitz M, Reuhl K, Perry B, Chan PH, Inouye M and Mirochnitchenko O. Overexpression of human glutathione peroxidase protects transgenic mice against focal cerebral ischemia/reperfusion damage. Brain Res Mol Brain Res 1998; 53: 333-338.
[33] Godar RJ, Ma X, Liu H, Murphy JT, Weinheimer CJ, Kovacs A, Crosby SD, Saftig P and Diwan A. Repetitive stimulation of autophagy-lysosome machinery by intermittent fasting preconditions the myocardium to ischemia-reperfusion injury. Autophagy 2015; 11: 1537-1560.
[34] Burne-Taney MJ, Ascon DB, Daniels F, Racusen L, Baldwin W and Rabb H. B cell deficiency confers protection from renal ischemia reperfusion injury. J Immunol 2003; 171: 3210-3215.